Diagonal Walking Strategy on Inclined Floor with Orientation Based Inverse Kinematics for Biped Robot

Fariz Ali and Atsuo Kawamura

***Abstract*— In this paper, diagonal walking strategy on inclined floor is proposed. In conventional methods, bipedal robots walking on inclined floor are solved only in straight direction. When a biped walks on flat floor, the pelvis orientation is always parallel with the floor surface. However, walking on inclined floor will make the robot pelvis tilts. Furthermore, in diagonal walking direction, the robot tilts in roll and pitch directions. In this paper, the problem is solved with orientation based inverse kinematics. Roll and pitch orientations of the pelvis are calculated to realize the diagonal walking on inclined floor. Center of mass trajectory is obtained by using linear inverted pendulum mode. The proposed method is validated via simulations by using a 3-D robot computer simulator known as ROCOS.**

***Index Term*— bipedal robot, diagonal walking, kinematics, orientation, robot computer simulator**

I. Introduction

THERE are many researches in bipedal robot walking field in the past 30 years. Unlike mobile robots with wheels, dynamical equilibrium motion is very difficult to be achieved by bipedal robots. Stable support polygon area of biped robot is very small which is bounded by one foot during single support phase or two feet in double support phase. Therefore, many researchers proposed various ideas related to stability indicator of walking [1]-[4].

A humanoid robot is intended to work in human surroundings. A number of researchers have investigated research problems for walking on stairs [5]-[9] and uneven surface [10]-[13]. There are also a number of papers for biped robot researches on turning motion [14]-[21].

Besides walking on stairs and uneven floor, inclined floor is also common in human environment. Therefore, slope walking is also important to be achieved. Biped walking on slope has started as early as in 1990 by Zheng and Shen [22]. In [22], the researchers have proposed a motion scheme for slope walking that consisted of three major aspects. The major aspects are solutions related to inclination of landing foot and gradient of the slope, slope motion scheme and transitional walking. Kim et al. proposed many control schemes for biped walking on slope such as upright pose, landing angular momentum, landing shock absorber, landing timing and landing position controls [23]. Huang et al. [24] proposed a motion pattern generator for slope walking in 3D dynamics by using preview control of zero moment point (ZMP). There are also researchers who implemented tactile sensing system to a humanoid robot for walking on the slopes [25]. The tactile sensors are installed on two robotic feet.

However, in all researches mentioned above, the walking is only done in straight direction on the inclined floor. The problems and difficulties of walking in diagonal walking on inclined floor are not considered in their papers. Therefore, in this paper, diagonal walking method on inclined floor is proposed. The general idea of diagonal walking is explained in section II. The bipedal robot platform used in simulations is introduced in section III. In section IV, the walking pattern with linear inverted pendulum mode (LIPM) is explained. The main contribution of this paper, which is the proposed method, is explained in section V. In section VI, results of simulations are presented and finally conclusion in section VII.

II. Diagonal Walking

Walking in straight direction on inclined floor are done and investigated in many research papers in the past. However, if the direction of the biped robot is not straight to the direction of the inclined floor but rotated slightly to the left or right, this is known as diagonal walking as shown in Fig. 1. Diagonal walking on inclined floor requires orientation input in roll and pitch directions of the waist with respect to the foot. Yaw orientation is maintained as it is. The details of the calculations and derivations are explained in section V, the proposed method section.

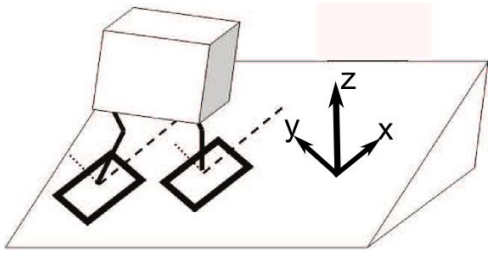

Fig. 1. Diagonal walking on inclined floor concept.

This work was supported in part by the Yokohama National University research grant.

Mr. Fariz Ali is a PhD student while Atsuo Kawamura is a full professor at the Department of Electrical and Computer Engineering Faculty of Engineering, Yokohama National University. The corresponding author can be contacted via e-mail: farizali@kawalab.dnu.ac.jp or farizaliynu@gmail.com.

III. BIPEDAL ROBOT PLATFORM

We have developed a bipedal robot called MARI-3 [26] to explore fast walking, running and jumping dynamics. The mechanical specifications of MARI-3 are summarized in Table I. MARI-3 has total of 13 DOF (degrees of freedom). Each leg has 6 DOF and 1 DOF at the waist for undesired yaw moment compensation. Furthermore, it is equipped with 6 axis Force/Torque sensors at the ankles. Plus, MARI-3 has a 3 axis rate gyro sensor and a 3 axis accelerometer at the pelvis. In its electronic hardware structure, the main controller is a 32 bit built-in Renesas SH-4 microcontroller. Data communication is performed via RON (RObot Network) bus which is a serial communication bus system, developed in our laboratory. Fig. 2 and Fig. 3 show the actual robot and its ROCOS [27] (RObot COntrol Simulator) simulation model. ROCOS is a 3-D dynamic simulator, also developed in or laboratory.

TABLE I
MECHANICAL SPECIFICATIONS OF MARI-3

Size	Upper leg length: 300 [mm]
	Lower leg length: 300 [mm]
	Ankle-sole length: 220 [mm]
Weight	Each leg: 13.477 [kg]
	Upper body: 6.683 [kg]
	Total: 33.64 [kg]

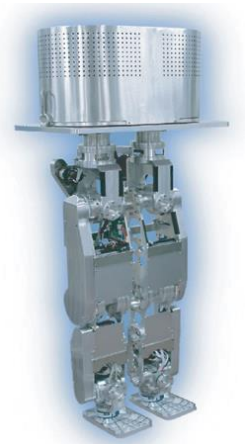

Fig. 2. MARI-3.

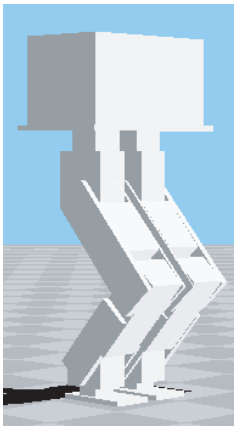

Fig. 3. ROCOS model.

IV. WALKING PATTERN WITH LIPM

Kajita et al. proposed LIPM for modeling a biped walking pattern generation [28]. In this paper, the same method is used to get the trajectories of center of mass (CoM) during the single support phase.

A. Single Support Phase

During the single support Phase, the LIPM approach is considered to get the relation between CoM and ZMP trajectories. CoM or the z height is always at a constant height with the slope surface and the equation is given as in (1).

$$z(t) = k_x x(t) + k_y y(t) + z_f \quad (1)$$

In (1) the k_x and k_y are the gradient of the slope surface in x and y directions respectively. The z_f is the CoM height used during walking on the flat floor surface.

The ZMP equations used during the single support phase are given as

$$x_{zmp} = x - \frac{\ddot{x}}{g} z \quad (2)$$

$$y_{zmp} = y - \frac{\ddot{y}}{g} z \quad (3)$$

where x_{zmp}, y_{zmp}, x, y, g and z denote the ZMP in x direction, ZMP in y direction, CoM trajectory in x direction, CoM trajectory in y direction, gravity and CoM trajectory in z direction. Furthermore, in order to use (2) and (3), these ZMP equations are solved analytically as shown in (4) and (5).

$$x(t) = (x_0 - x_{zmp})\cosh(\omega t) + \frac{\dot{x}_0}{\omega}\sinh(\omega t) + x_{zmp} \quad (4)$$

$$y(t) = (y_0 - y_{zmp})\cosh(\omega t) + \frac{\dot{y}_0}{\omega}\sinh(\omega t) + y_{zmp} \quad (5)$$

$$\omega = \sqrt{\frac{g}{z}}$$

Here, x_0 and y_0 denote the initial trajectory of CoM in x and y directions respectively.

B. Double Support Phase

During the double support phase, the CoM trajectories are ensured to be connected smoothly by using 5th polynomial as in (6)-(8).

$$p(t) = a_0 + a_1 t + a_2 t^2 + a_3 t^3 + a_4 t^4 + a_5 t^5 \quad (6)$$

$$v(t) = a_1 + 2a_2 t + 3a_3 t^2 + 4a_4 t^3 + 5a_5 t^4 \quad (7)$$

$$a(t) = 2a_2 + 6a_3 t + 12a_4 t^2 + 20a_5 t^3 \quad (8)$$

Here, p, v and a denote the position, velocity and acceleration respectively. a0 to a5 are determined with six constraints which are initial and ending of position, velocity and acceleration.

V. PROPOSED METHOD

A. Proposed Kinematics

In our method we proposed kinematics that included positions and orientations. For position vectors, CoM position and swing leg position are used. While for orientation, pelvis orientations with respect to the support foot are used.

CoM and Swing Foot Positions

In our method, right foot is used as reference. Therefore, the CoM position and the swing foot position are always referred to the right foot sole center as shown in Fig. 4. Some of biped researchers used pelvis as reference point and used it as input trajectory. This is because it is visible and easier to visualize than the CoM point. However, the authors believed that

position of CoM is more accurate to be used as input trajectory since ZMP equations calculated earlier in (2)-(5) are related to CoM position point.

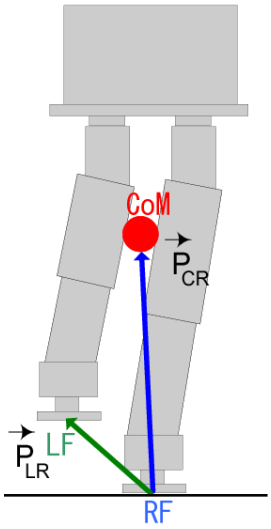

Fig. 4. Single support phase.

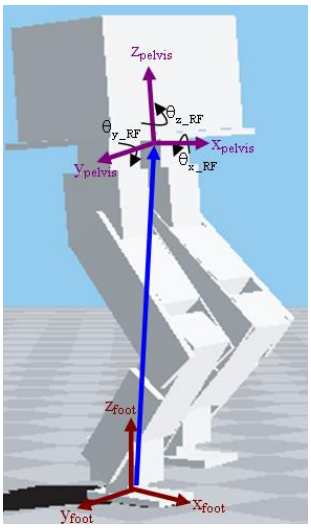

Fig. 5. Pelvis orientation.

A position of robot during right foot's single support phase is shown in Fig. 4. From the figure, $\vec{\mathbf{P}}_{\mathbf{CR}}$ and $\vec{\mathbf{P}}_{\mathbf{LR}}$ are the position vectors from the right foot to the CoM, and the right foot to the left foot, respectively. ZMP equations are used to determine $\vec{\mathbf{P}}_{\mathbf{CR}}$, while $\vec{\mathbf{P}}_{\mathbf{LR}}$ is generated from swing leg motion. From these 6 existing position vectors, the forward kinematics (FK) equations are determined. These functions contain the joint angles variables as shown in (9).

$$\vec{p}_i = f_i(q_1,...,q_{12}) \quad i = 1,...,6 \tag{9}$$

From the position vectors, there are six equations and twelve joint angles variables. In order to avoid redundancy, another six equations are required. These additional equations are obtained from orientation equations which will be explained further in the next subsection. In (9) and other equations later, q symbolizes the joint angles. The left foot's single support phase solution is not provided but it can be solved in the same way.

Pelvis Orientation

Fig.5 shows the pelvis orientation with respect to the right foot. $\theta_{x\text{-}RF}$, $\theta_{y\text{-}RF}$ and $\theta_{z\text{-}RF}$ represents roll, pitch and yaw rotations with respect to the foot frame which is located in the middle of right foot sole.

In order to derive the expressions for the pelvis orientation, the basic rotation matrices around x, y and z-axes must be obtained first [29]. Multiplication all of the basic rotation matrices in x-y-z Euler sequence, gives a 3x3 matrix in functions of $\theta_{x\text{-}RF}$, $\theta_{y\text{-}RF}$ and $\theta_{z\text{-}RF}$ as shown in (10).

$$R_x \times R_y \times R_z = \begin{bmatrix} M_{11} & M_{12} & M_{13} \\ M_{21} & M_{22} & M_{23} \\ M_{31} & M_{32} & M_{33} \end{bmatrix}$$

Where,

$$\begin{aligned}
M_{11} &= \cos(\theta_{y_RF})\cos(\theta_{z_RF}) \\
M_{12} &= -\cos(\theta_{y_RF})\sin(\theta_{z_RF}) \\
M_{13} &= \sin(\theta_{y_RF}) \\
M_{21} &= \sin(\theta_{x_RF})\sin(\theta_{y_RF})\cos(\theta_{z_RF}) + \\
&\quad \cos(\theta_{x_RF})\sin(\theta_{z_RF}) \\
M_{22} &= -\sin(\theta_{x_RF})\sin(\theta_{y_RF})\sin(\theta_{z_RF}) + \\
&\quad \cos(\theta_{x_RF})\cos(\theta_{z_RF}) \\
M_{23} &= -\sin(\theta_{x_RF})\cos(\theta_{y_RF}) \\
M_{31} &= -\cos(\theta_{x_RF})\sin(\theta_{y_RF})\cos(\theta_{z_RF}) + \\
&\quad \sin(\theta_{x_RF})\sin(\theta_{z_RF}) \\
M_{32} &= \cos(\theta_{x_RF})\sin(\theta_{y_RF})\sin(\theta_{z_RF}) + \\
&\quad \sin(\theta_{x_RF})\cos(\theta_{z_RF}) \\
M_{33} &= \cos(\theta_{x_RF})\cos(\theta_{y_RF})
\end{aligned} \tag{10}$$

From the transformation matrix of the pelvis with respect to the right foot, the orientation in term of joint angle q_1 to q_6 is obtained as shown in (11). Value of '*a*' in these equations is, $a = q_3 + q_4 + q_5$. Notice that only q_1 to q_6 are appeared here since the joints angles involved are contributed from right leg only. The left leg case can be solved in the same manner.

$${}^{\text{Right Foot}}_{\text{Pelvis}}R = \begin{bmatrix} N_{11} & N_{12} & N_{13} \\ N_{11} & N_{11} & N_{11} \\ N_{11} & N_{11} & N_{11} \end{bmatrix}$$

Where,

$$\begin{aligned}
N_{11} &= \sin(a)\sin(q_1)\sin(q_2) + \cos(a)\cos(q_1) \\
N_{12} &= -\sin(a)\cos(q_1)\sin(q_2) + \cos(a)\sin(q_1) \\
N_{13} &= \sin(a)\cos(q_2) \\
N_{21} &= -\sin(q_6)\sin(a)\sin(q_1) - \cos(q_6)\sin(q_1)\cos(q_2) + \\
&\quad \sin(q_6)\cos(a)\sin(q_1)\sin(q_2) \\
N_{22} &= -\sin(q_6)\sin(a)\sin(q_1) - \sin(q_6)\cos(a)\cos(q_1)\sin(q_2) + \\
&\quad \cos(q_6)\cos(q_1)\cos(q_2) \\
N_{23} &= \sin(q_6)\cos(a)\cos(q_2) + \sin(q_2)\cos(q_6) \\
N_{31} &= \cos(q_6)\cos(a)\sin(q_1)\sin(q_2) - \cos(q_6)\sin(a)\cos(q_1) + \\
&\quad \sin(q_6)\sin(q_1)\cos(q_2) \\
N_{32} &= -\cos(q_6)\sin(a)\sin(q_1) - \sin(q_6)\cos(q_1)\cos(q_2) - \\
&\quad \cos(a)\cos(q_6)\cos(q_1)\sin(q_2) \\
N_{33} &= \cos(q_6)\cos(a)\cos(q_2) - \sin(q_2)\sin(q_6)
\end{aligned} \tag{11}$$

Each element of matrix in (11) is then compared with each element of matrix in (10). The equations are solved to obtain the FK orientation expressions for the pelvis with respect to right foot as shown in (12)-(14).

$$\theta_{x\_RF} = \arctan\left[\frac{-\sin(q_6)\cos(a)\cos(q_2) - \sin(q_2)\cos(q_6)}{\cos(q_6)\cos(a)\cos(q_2) - \sin(q_2)\sin(q_6)}\right] \tag{12}$$

$$\theta_{y\_RF} = \arcsin\left[\sin(a)\cos(q_2)\right] \quad (13)$$

$$\theta_{z\_RF} = \arctan\left[\frac{\sin(a)\cos(q_1)\sin(q_2) - \cos(a)\sin(q_1)}{\sin(a)\sin(q_1)\sin(q_2) + \cos(a)\cos(q_1)}\right] \quad (14)$$

Where '*a*' in (12)-(14) is the same as in (11). For the left leg case, the FK orientation equations, $\theta_{x\text{-}LF}$, $\theta_{y\text{-}LF}$ and $\theta_{z\text{-}LF}$ are obtained in the same approach to obtain (12)-(14).

Inverse Kinematics

In order to solve the inverse kinematics (IK), sufficient numbers of FK equations are needed. CoM position is chosen as the input trajectory instead of pelvis joint for a more accurate dynamics representations. From position vector, six position equations and twelve joint angles variables as shown in (9) previously can be obtained. Another six more equations are contributed from the orientation.

Pelvis orientation with respect to the foot sole is selected to obtain the IK. With six more equations from the orientation, there are sufficient number of equations and solvable variables.

One of the popular methods to solve the IK in robot study is by using a Jacobian based method. There are twelve joint angles variables from q_1 to q_{12}. Let assigned the joint angles as in (15), while positions and orientations as in (16).

$$\vec{Q} = \left[q_1\ q_2\ q_3\ q_4\ q_5\ q_6\ q_7\ q_8\ q_9\ q_{10}\ q_{11}\ q_{12}\right]^T_{12x1} \quad (15)$$

$$\vec{P} = \left[P_{CR}\ \ P_{LR}\ \ \theta_R\ \ \theta_L\right]^T_{12x1}$$

Where,

$$\theta_R = \left[\theta_{x\_RF}\ \ \theta_{y\_RF}\ \ \theta_{z\_RF}\right]^T_{3x1} \quad (16)$$

$$\theta_L = \left[\theta_{x\_LF}\ \ \theta_{y\_LF}\ \ \theta_{z\_LF}\right]^T_{3x1}$$

By having (15) and (16), a Jacobian matrix between these two equations is defined as in (17).

$$\dot{\vec{P}} = J\,\dot{\vec{Q}} \quad (17)$$

Avoiding the singularities, (17) could be solved by using Newton-Raphson Method [30].

B. *Trajectory Planning Procedure*

The trajectory planning procedures are summarized into several steps. The procedures are described as follows:

1) *Calculation of the CoM position trajectory and the foot swing position trajectory.*
2) *Calculation of roll and pitch joint angles for diagonal walking on inclined floor.*

The details of the procedures above are explained as following.

Calculation of the CoM position trajectory and the foot swing trajectory.

The CoM position is designed by using LIPM approach as explained in section IV. During the single support phase, equation (4) and (5) are used in order to get the CoM x and y trajectories while maintaining the ZMP to be inside the support polygon. During the single support phase, the support polygon is bounded by the size of the support foot. When the CoM traveled in single support phase, foot swing will move to make a step. This swing foot is moved by using polynomial function.

In double support phase smooth connections between two phases are ensured by using a 5th polynomial function as given in (6) – (8). Position, velocity and acceleration are taken into account in order to get smooth movement or transition between phases.

It is noticed that the ZMP equations as shown in (2) and (3) are valid for flat floor and inclined floor as well. This has been explained by Sato in his paper [5].

Calculation of roll and pitch joint angles for diagonal walking on inclined floor.

Besides the positions, pelvis orientations must be designed according to the floor surface. If the floor is flat, all the orientation input trajectories, $\theta_{x\text{-}RF}$, $\theta_{y\text{-}RF}$, $\theta_{z\text{-}RF}$, $\theta_{x\text{-}LF}$, $\theta_{y\text{-}LF}$ and $\theta_{z\text{-}LF}$ are all zero. However, on the inclined floor these orientation input trajectories are not zero. $\theta_{x\text{-}RF}$ and $\theta_{x\text{-}LF}$ denote the roll orientation of the pelvis with respect to right foot and left foot respectively. $\theta_{y\text{-}RF}$ and $\theta_{y\text{-}LF}$ denote the pitch orientation of the pelvis with respect to right foot and left foot respectively. Furthermore, $\theta_{z\text{-}RF}$ and $\theta_{z\text{-}LF}$ denote the yaw orientation of the pelvis with respect to right foot and left foot respectively.

Diagonal walking is occurred when the biped robot rotated to right or left from the straight orientation on inclined floor as shown in Fig. 6. In this research, the inclined floor is assumed known. If the slope angle of the inclined floor is known, it is important to know the relationship between the slope and the pitch angles. Later on, relationship between pitch and roll joints are determined.

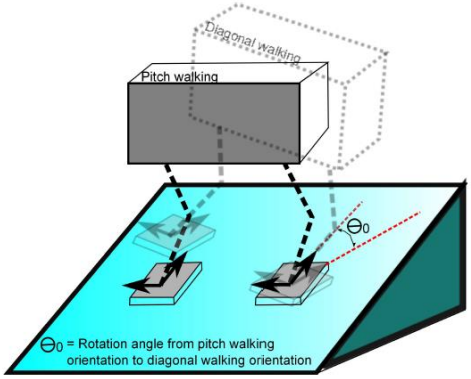

Fig. 6. Diagonal walking on inclined floor.

The derivations of relation between slope and pitch angles can be obtained by using Fig. 7 as reference. Θ_0 is the angle when the biped robot rotated to the right from its straight

position to perform a diagonal walking position.

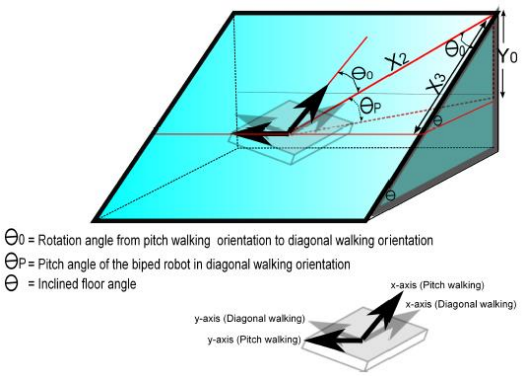

Fig. 7. Relation between slope and pitch angles.

The derivations are shown in (18) – (20).

$$Y_0 = \sin(\theta_p) \times X_2 = \sin(\theta) \times X_3 \tag{18}$$

$$\sin(\theta_p) = \sin(\theta) \times \frac{X_3}{X_2} \tag{19}$$

$$\sin(\theta_p) = \sin(\theta) \times \cos(\theta_0) \tag{20}$$

It is shown in derivations above, the relationship between pitch and slope angles as shown in (20).

On the other hand, the derivations of relation between roll and pitch angles are obtained by using Fig. 8 as reference.

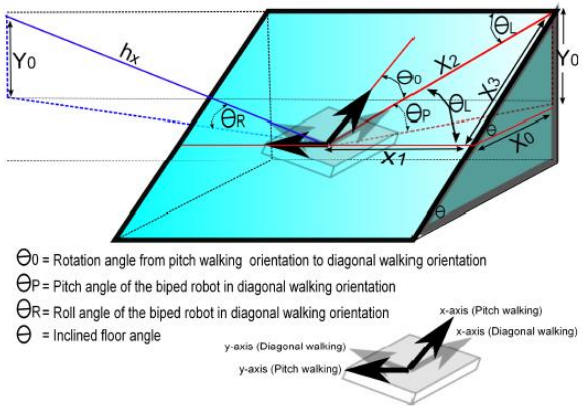

Fig. 8. Relation between roll and pitch angles.

The derivations between roll and pitch angles are shown in (21) – (28).

$$X_3 = \frac{Y_0}{\sin(\theta)} \tag{21}$$

$$X_2 = \sqrt{X_1^2 + \left(\frac{Y_0}{\sin(\theta)}\right)^2} \tag{22}$$

$$\sin(\theta_p) = \frac{Y_0}{X_2} = \frac{Y_0}{\sqrt{X_1^2 + \left(\frac{Y_0}{\sin(\theta)}\right)^2}} \tag{23}$$

$$\tan(\theta_L) = \frac{h_x}{X_2} \tag{24}$$

$$h_x = \tan(\theta_L) \times \sqrt{X_1^2 + \left(\frac{Y_0}{\sin(\theta)}\right)^2} \tag{25}$$

$$\sin(\theta_R) = \frac{Y_0}{h_x} = \frac{Y_0}{\tan(\theta_L) \times \sqrt{X_1^2 + \left(\frac{Y_0}{\sin(\theta)}\right)^2}} \tag{26}$$

Equ. (23), (24) and (26) are then compared. As the result, (27)-(28) are obtained as below.

$$\sin(\theta_p) = \sin(\theta_R) \times \tan(\theta_L) \tag{27}$$

$$\sin(\theta_p) = \sin(\theta_R) \times \tan(90^0 - \theta_0) \tag{28}$$

It is shown in the derivations above, the relationship between pitch and roll angles as shown in (28).

VI. SIMULATIONS

The simulations are done by using ROCOS. The simulations setup parameters are shown in Table 2. In these simulations, the biped is walking on floor in diagonal direction.

TABLE II
SIMULATIONS PARAMETERS

Maximum height of swing leg [m]	0.03
Forward foot stride [m]	0.07
Perpendicular of CoM height to slope surface [m]	0.4971
Single support time [s]	0.6
Double support time [s]	0.8
Inclined floor angle, Θ [^{0}]	7.08
Roll orientation angle, Θ_R [^{0}]	5
Pitch orientation angle, Θ_p [^{0}]	5
Rotation from the straight, Θ_0 [^{0}]	45

As shown in the Table II, the diagonal walking simulations are done for the inclined floor with slope angle of 7.08 degree. If the floor slope angle, Θ and the rotation from straight, Θ_0 are known, the roll and pitch joint angles can be calculated by using (20) and (28). It is also given that the Θ_0 is 45 degree.

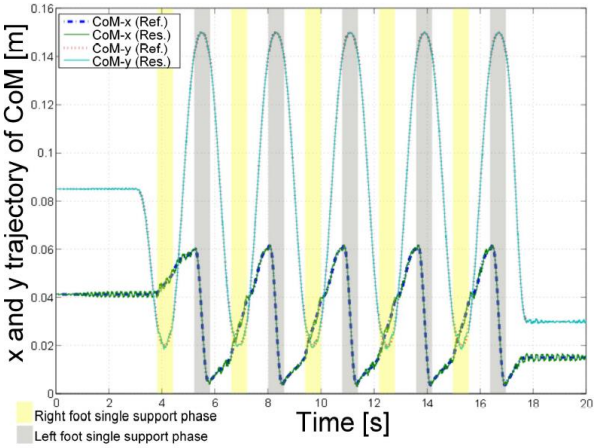

Fig. 9. x and y trajectory of CoM.

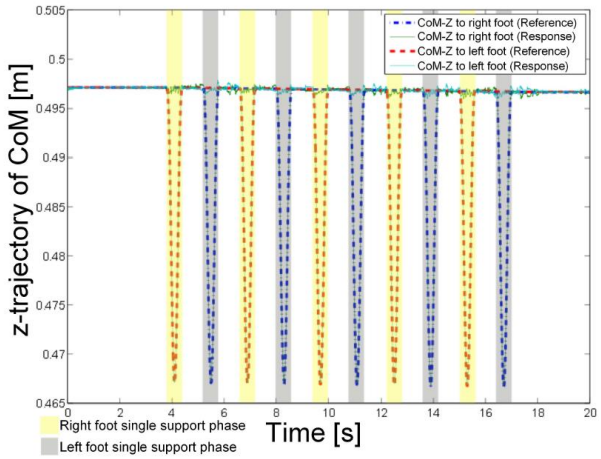

Fig. 10. z trajectory of CoM.

In this simulation, the biped robot performed a ten steps walking in diagonal direction on the inclined floor. The CoM trajectories in x, y and z directions are plotted and shown as in Fig. 9 and 10. The perpendicular distance of the CoM height in z direction between the CoM and the support foot is always constant at 0.4971m as shown in Fig. 10. It can be seen that smooth CoM trajectories are obtained by using the proposed method as confirmed in Fig. 9 and 10.

The value of Θ_0 is 45 degree and the inclined floor slope angle is 7.08 degree. Using (20) the pitch orientation is obtained as (29).

$$\sin(\theta_p) = \sin(\theta) \times \cos(\theta_0)$$
$$\sin(\theta_p) = \sin(7.08^0) \times \cos(45^0)$$
$$\therefore \theta_p = 5^0 \quad (29)$$

Furthermore, the roll orientation is determined by using (28) as shown in (30).

$$\sin(\theta_p) = \sin(\theta_R) \times \tan(90^0 - \theta_0)$$
$$\sin(5^0) = \sin(\theta_R) \times \tan(90^0 - 45^0)$$
$$\therefore \theta_R = 5^0 \quad (30)$$

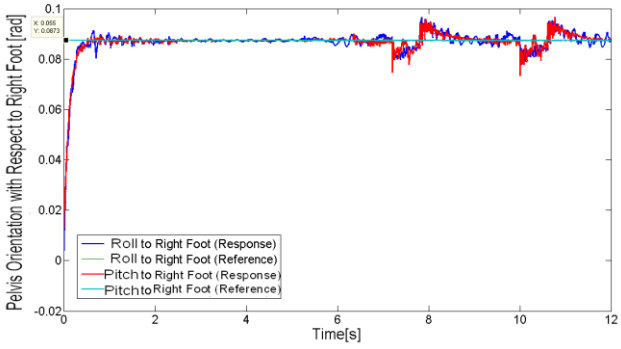

Fig. 11. Pelvis orientation with respect to right foot.

The roll and pitch orientation of the pelvis with respect to the right foot is shown as in Fig. 11. With the proposed method, the positions and orientations are determined and the diagonal walking is achieved successfully.

VII. Conclusion

In this paper, a diagonal walking strategy on inclined floor is proposed. In the procedure, position and orientation based inverse kinematics is proposed in order to get the roll and pitch orientations of the pelvis systematically. Furthermore, roll, pitch and slope angle relationships are derived and shown in this paper. The proposed method is confirmed by using a 3D robot computer simulator known as ROCOS. The proposed method can be extended for biped turning motion on inclined floor. Furthermore, it is intended to support the theoretical and simulations explained in this paper by performing experiment using MARI-3 biped robot in the future.

References

[1] M. Vukabrotovic and B. Borovac, "Zero-moment point – thirty five years of its life," in *Int. Journal of Humanoid Robotics*, vol. 1, no. 1, pp. 157–173, 2004.

[2] H. Hirukawa, S. Hattori, K. Harada, S. Kajita, K. Kaneko, F. Kanehiro, K. Fujiwara and M. Morisawa, "A universal stability criterion of the foot contact of legged robots – adios ZMP," in *IEEE Int. Conf. on Robotics and Automation*, Orlando, 2006, pp. 1976–1983.

[3] A. Goswami "Foot Rotation Indicator (FRI) point: a new gait planning tool to evaluate postural stability of biped robots," in *IEEE Int. Conf. on Robotics and Automation*, Detroit, 1999, pp. 47–52.

[4] S. Takao, Y. Yokokohji and T. Yoshikawa "FSW (Feasible Solution of Wrench) for multi-legged robots," in *IEEE Int. Conf. on Robotics and Automation*, Taipei, 2003, pp. 3815–3820.

[5] T. Sato, S. Sokaino, E. Ohashi and K. Ohnishi, "Walking trajectory planning on stairs using virtual slope for biped robots," *IEEE Trans. On Industrial Electronics*, vol. 58, no. 4, pp. 1385–1396, 2001.

[6] K. S. Jeon, O. Kwon and J. H. Park "Optimal trajectory generation for a biped robot walking a staircase based on genetic algorithms," in *IEEE/RSJ Int. Conf. on Intelligent Robots and Systems*, Sendai, 2004, pp. 2837–2842.

[7] C. Fu and K. Chen, "Gait synthesis and sensory control of stair climbing for a humanoid robot," *IEEE Trans. On Industrial Electronics*, vol. 55, no. 5, pp. 2111–2120, 2008.

[8] G. Capi, Y. Nasu, L. Barolli, K. Mitobe and K. Takeda, "Application of genetic algorithms for biped robot gait synthesis optimization during walking and going-up stairs," *Advanced Robotics*, vol. 15, no. 6, pp. 675–694, Apr. 2001.

[9] P. Michel, J. Chestnutt, S. Kagami, K. Nishiwaki, J. Kuffner and T. Kanade "GPU-accelerated real-time 3D tracking for humanoid

locomotion and stair climbing," in *IEEE/RSJ Int. Conf. on Intelligent Robots and Systems*, California, 2007, pp. 463–469.
[10] S. Kajita, M. Morisawa, K. Harada, K. Kaneko, F. Kanehiro, K. Fujiwara and H. Hirukawa "Biped walking pattern generator allowing auxiliary ZMP control," in *IEEE/RSJ Int. Conf. on Intelligent Robots and Systems*, Beijing, 2006, pp. 2993–2999.
[11] T. Erez and W. D. Smart "Bipedal walking on rough terrain using manifold control," in *IEEE/RSJ Int. Conf. on Intelligent Robots and Systems*, San Diego, 2007, pp. 1539–1544.
[12] C. L. Shih and C. J. Chiou, "The motion control of a statically stable biped on uneven floor," *IEEE Trans. On Syst., Man, and Cybernatics, Part B: Cybernatics* vol. 28, no. 2, pp. 244–249, 1998.
[13] T. Sato, S. Sakaino and K. Ohnishi, "Stability index for biped robot moving on rough terrain," *IEEJ Trans. On Industrial Applications*, vol. 129, no. 6, pp. 571–577, 2009.
[14] M. Yagi and V. Lumelsky, "Biped robot locomotion in scenes with unknown obstacles," in *IEEE Int. Conf. on Robotics and Automation*, Detroit, 1999, pp. 375–380.
[15] M. Yagi and V. Lumelsky "Synthesis of turning pattern trajectories for a biped robot in a scene with obstackes," in *IEEE/RSJ Int. Conf. on Intelligent Robots and Systems*, Takamatsu, 2000, pp. 1161–1166.
[16] S. Kajita, F. Kanehiro, K. Kaneko, K. Fujiwara, K. Yokoi and H. Hirukawa, "Biped walking pattern generation by a simple three-dimensional inverted pendulum model," *Advanced Robotics*, vol. 17, no. 2, pp. 131–147, 2003.
[17] S. Kajita, F. Kanehiro, K. Kaneko, K. Fujiwara, K. Harada, K. Yokoi and H. Hirukawa, "Biped walking pattern generation by using preview control of zero-moment point," in *IEEE Int. Conf. on Robotics and Automation*, Taipei, 2003, pp. 1620–1626.
[18] S. Aoi, K. Tsuchiya and K. Tsujita, "Turning control of a biped locomotion robot using nonlinear oscillators," in *IEEE Int. Conf. on Robotics and Automation*, New Orleans, 2004, pp. 3043–3048.
[19] Z. Thang, Z. Sun, H. Liu and M. J. Er, "Clock-turning gait synthesis for humanoid robots ," in *Journal of Control Theory and Applications*, vol. 5, no. 1, pp. 23–27, 2007.
[20] M. T. Farrell and H. Herr "Angular momentum primitives for human turning: control implications for biped robots," in *IEEE/RAS Int. Conf. on Humanoid Robots*, Daejeon, 2008, pp. 163–167.
[21] I. W. Park, J. Y. Kim and J. H. Oh, "Online walking pattern generation and its application to a biped humanoid robot-KHR-3(HUBO)," *Advanced Robotics*, pp. 159–190, 2008.
[22] Y. F. Zheng and J. Shen, "Gait synthesis for the SD-2 biped robot to climb sloping surface," in *IEEE Trans. On Robotics and Automation*, vol. 6, no. 1, pp. 86–96, 1990.
[23] J. Y. Kim, I. W. Park and J. H. Oh, "Walking control algorithm of biped humanoid robot on uneven and inclined floor," in *Journal of Intelligent and Robotic Systems*, vol. 48, no. 4, pp. 457–484, 2007.
[24] W. Huang, C. M. Chew, Y. Zheng and G. S. Hong "Pattern generation for bipedal walking on slopes and stairs," in *IEEE/RAS Int. Conf. on Humanoid Robots*, Daejeon, 2008, pp. 205–210.
[25] K. Suwanratchatamanee, M. Matsumoto and S. Hashimoto "Walking on the slopes with tactile sensing system for humanoid robot," in *Int. Conf. on Control, Automation and Systems*, Gyeonggi-do, 2010, pp. 350–355.
[26] A. Kawamura and C. Zhu, "The development of biped robot MARI-3 for fast walking and running," in *IEEE/RAS Int. Conf. on Humanoid Robots*, Genova, 2006, pp. 559-604.
[27] Y. Fujimoto and A. Kawamura, "Simulation of an autonomous biped walking robot including environmental force interaction," in *IEEE Robotics and Automations Magazine*, vol.5, no.2, pp. 33-42, 1998.
[28] S. Kajita, F. Kanehiro, K. Kaneko, K. Yokoi and H. Hirukawa, "The 3D linear inverted pendulum mode: a simple modeling for a biped walking pattern generation," in *IEEE/RSJ Int. Conf. on Intelligent Robots and Systems*, Maui, 2001, pp. 239–246.
[29] J.J. Craig, Introductions to Robotics: Mechanics and Control 3nd Edition, Prentice Hall, 2004.
[30] W.H. Press, S. A. Teukolsky, W.T. Vatterling, and B.P. Flannery Numerical Recipes in c: The Art of Scientific Computing 2nd Edition, Cambridge University Press, 1992.